# Journal of Materials Chemistry C

Accepted Manuscript


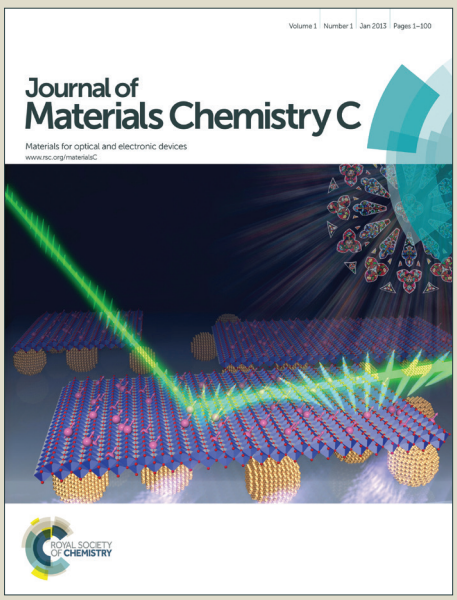





ROYAL SOCIETY OF CHEMISTRY

www.rsc.org/materialsC

Journal of
Materials Chemistry C

RSCPublishing

PAPER

# Dielectric and optical anisotropy enhanced by 1,3-dioxolane terminal substitution on tolane-liquid crystals†

Cite this: DOI: 10.1039/x0xx00000x

Received 00th January 2015,
Accepted 00th January 2015

DOI: 10.1039/x0xx00000x

www.rsc.org/MaterialsC

Ran Chen,[a] Yi Jiang,[b] Jian Li,[c] Zhongwei An,[*a,c] Xinbing Chen[a] and Pei Chen[a]

Four series of 1,3-dioxolane-terminated liquid crystals were prepared *via* multi-step reactions based on 4-alkylcyclohexanecarboxylic acids. Their structures were confirmed by infrared spectrometry (IR), nuclear magnetic resonance (NMR) and mass spectra (MS). Their properties were measured by differential scanning calorimetry (DSC), polarising optical microscopy (POM), X-ray diffraction (XRD), Abbe refractometer and electrical constants instrument. The results show that the positive dielectric anisotropy and birefringence of the tolane-liquid crystals are increased significantly by an introduction of the 1,3-dioxolane as a terminal group. The application of 1,3-dioxolane-terminated liquid crystals in the mixture was investigated and the results show that lower threshold voltage, wider nematic range and higher birefringence are obtained by comparison with that containing the liquid crystals with a buty-3-enyl as terminal. The lateral fluoro substituent, alkyne-bridge and 1,3-dioxolane terminal group enhance the stability of the nematic mesophase and solubility of the corresponding compounds in the common host liquid crystal mixture. Meanwhile, DFT calculations of dipole moments, molecular polarizabilities were used to correlate the experimental findings.

## Introduction

Liquid crystal displays(LCDs) have become wide spread information terminals because of their low driving voltages and power consumptions, small sizes and portable conveniences. The huge market requirements of mobile electronics are always the main driving force of LCDs technology, which was initiated by the caculators and game players, further development of the technology to achieve the protable devices, such as notebook, personal digital assistants.[1] The wearable electronic devices are realized nowadays and are potential for the future market.[2] The large dielectric and optical anisotropy of liquid crystal materials have been intensively requested with the progress of LCDs technology. Therefore, the enhancement of the dielectric and optical anisotropy has been one of the attractively hot points and great challenges in the field of liquid crystal materials.

Various design concepts[3,4] have been proposed to arrange the synthons for better properties. During the past decades, to obtain high positive dielectric anisotropy ($\Delta\varepsilon$), three available strategies involved the use of: (1) extremely polar fluorinated terminal groups, such as F, $CF_3$ or $OCF_3$;[5] (2) intrinsically polar bridge structures, such as $CF_2O$ bridges;[6] (3) polar aliphatic oxygen heterocycles, such as 1,3-dioxane and tetrahydropyran structures.[7,8] Strategy (1) or (2) was used alone to favour dielectric anisotropy but decrease the molecular aspect ratio, which directly results in a limiting or no liquid crystalline phase interval. Although, the introduction of phenyl rings can increase the molecular long axis and broaden the mesophase range, the liquid crystal molecules possess poor solubility generally.[8] Besides, the complex synthetic route and limitation of structural scope diminish the applications of strategy (3) for variety of liquid crystal compounds.[8] Even though, all of the above strategies are still widely used in liquid crystal materials with a large positive $\Delta\varepsilon$.

Liquid crystals (LCs) containing heterocyclic rings are of crucial importance in the design and synthesis of novel advanced functional materials.[9,10] Among heterocyclic systems, 5-membered heterocyclic rings are of great importance as core units in thermotropic LCs due to their ability to impart lateral and longitudinal dipoles with alterations in molecular shape.[11] With the introduction of 5-membered heterocyclic ring structures into the liquid crystal

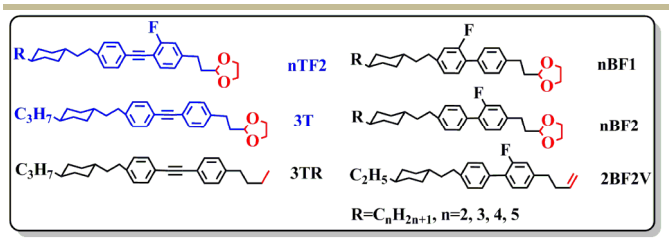


**Fig.1** The chemical structures of target compounds with the 1,3-dioxolane terminal group and reference compounds **nBF1**, **nBF2**, **3TR** and **2BF2V**.

molecules as a terminal group and comprehensive understanding its influences on the dielectric and optical anisotropy of the LCs, we have designed and prepared two series of 1,3-dioxolane-terminated tolane LCs, as shown in Fig. 1. To our surprise, the 1,3-dioxolane terminal group can effectively improve the positive dielectric anisotropy $\Delta\varepsilon$ and increase the birefringence compared with the same molecular skeleton, although our previous studies took the compounds with 1,3-dioxolane terminal as the liquid crystal intermediates to synthesize terminal alkenyl-based LCs.[12] Two series of compounds **nBF1** and **nBF2** reported by our group[12] were also synthesized for comparison (Fig. 1). Meanwhile, DFT calculations of dipole moments and molecular polarizabilities were used to correlate the experimental results.

## Experimental section

### 1. Materials

4-Alkylcyclohexanecarboxylic acids, 2-(4-bromophenethyl)-1,3-dioxolane, 2-(4-bromo-3-fluorophenethyl)-1,3-dio-xolane, were purchased from Xi'an Caijing Opto-Electrical Science Technology Co. Ltd. and used as received. Pd /C (5%), tetra butyl ammonium bromide (TBAB) and tetrakis (triphenylphosphine)-palladium ($Pd(PPh_3)_4$) were purchased from Aladdin-reagent Co. and used as received. Potassium hydroxide (KOH), petroleum ether (PE), ethyl acetate (EA), methylbenzene (PhMe), were purchased from Sinopharm Chemical Reagent Co. and used as received. Mixed liquid crystal (NR-5336LA) was purchased from Chisso Corporation. Compounds **1**, **2**, **2BF2V** and **3TR** were synthesized according to literature procedures.[12-14]

### 2. Characterization and measurements

The structures of the final products and intermediates were confirmed by a variety of spectral methods. IR spectra were recorded on a Nicolet Avatar360E spectrometer. $^1$H-nuclear and $^{13}$C-nuclear magnetic resonance ($^1$H NMR and $^{13}$C NMR), with TMS as internal standard, were recorded on a Bruker AV 300-MHz and 600-MHz instruments. The mass spectra were obtained by GC/EI-MS Thermo DSQ II with m/z 50 to 650. Elemental analysis was performed for C and H in an Elementar Vario EL III instrument (Elementar Analysensysteme GmbH, Hanau, Germany).

The phase transition temperatures were measured by Shimatsu DSC-60 under nitrogen atmosphere at the heating and cooling rate of 10 $^{o}$C min$^{-1}$, and POM, LEICA DM2500P with Linkam THMS600 hot-stage and control unit at a heating and cooling rate of 0.5 $^{o}$C min$^{-1}$. X-ray diffraction (XRD) was performed on the Bruker D8 ADVANCE X-ray diffractometer (Rheinstetten, Germany). The phase transition temperatures reported in this paper were the peak values of the transition on DSC curves. The birefringence ($\Delta n$) were measured at 20 °C by Abbe refractometer using a 589 nm wavelength light source in a mixed liquid crystal (NR-5336LA). The dielectric anisotropies ($\Delta\varepsilon$) of liquid crystal monomers were measured at 20 °C in the host mixture[15] by electrical constants instrument (EC-1, TOYO Corporation, Japan).

The dielectric constants ( $\varepsilon_{//}$ and $\varepsilon_{\perp}$) were measured by EC-1, the viscosity ($\gamma_1$) and elastic constant ($K_{11}$) were measured by Model 6254 (Multi Channel Liquid Crystal Evalution System, TOYO Corporation, Japan), the electro-optical properties ($V_{th}$, $T_r$ and $T_f$) were measured by LCT-5076E (North LCD Engineering R&D Center, China), the freezing point (Mp) was measured by Haier Ultralow Temperature Freezer DW-86W100.

### 3. Synthesis of compounds

The synthetic routes of compounds **nBF1**, **nBF2**, **nTF2** and **3T** are illustrated in Scheme 1. The compounds **nBF1** and **nBF2** were obtained by literature procedures reported in our previous paper [12]. The synthesis procedures of **nTF2** and **3T** are described below. The $^1$H NMR and $^{13}$C NMR spectra of target compounds **2TF2**, **3TF2**, **4TF2**, **5TF2** and **3T**, all characterized data are showed in the ESI† (see content 2).

**General synthesis procedure of nTF2 and 3T.**

Under nitrogen protection, a mixture of acetylenic alcohol **2** (6.4 mmol), KOH (52 mmol) and TBAB (0.6 mmol) in 40 mL of PhMe/$H_2O$ at a ratio of 4:1 (V/V) was stirred at 60 $^{o}$C for 30 min. Then the aryl bromide (5.8 mmol) and $Pd(PPh_3)_4$ (0.2 mmol) were added and the stirred mixture was heated at 80 $^{o}$C for 12 h. After the mixture was cooled to room temperature, the solution was filtered over a pad of silica gel. Then the mixture was diluted with water and extracted with ethyl acetate for three times. The combined organic phase was dried over $MgSO_4$. After removal of the solvent in *vacuo*, the residue was purified *via* column chromatography on silica gel using PE/EA (20/1) as eluent to give purity above 99% for HPLC measurement.

## Results and discussion

### Synthesis and characterization

The synthesis of target compounds **nTF2** and **3T**, was based on Sonogashira Hagihara reaction of different acetylenic alcohol and aryl bromide in one pot to give good over all yields of 45-55% with purities higher than 99% (HPLC). Our results show that this synthetic pathway is facile and efficient, which is beneficial to avoid contamination of chemical impurities. The structures of the products were characterized by IR, $^1$H NMR, $^{13}$C NMR, GC/EI-MS and elemental analysis. All these results confirmed the proposed structures of target compounds.

### Liquid crystal characterization

The mesomorphic properties of the obtained compounds were

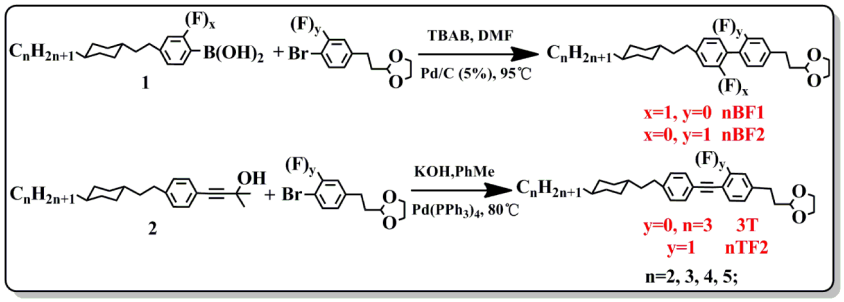


**Scheme 1** Synthetic routes of **nBF1**, **nBF2**, **nTF2** and **3T**.

determined by differential scanning calorimetry (DSC), polarizing optical microscopy (POM) and XRD method (see Fig. S6 in the ESI). The phase transition temperatures, the associate enthalpies and mesophase textures of the compounds **nBF1**, **nBF2**, **nTF2** and **3T** are summarized in Table S1. (see content 3 in the ESI) Fig. 2 summarizes the phase sequences and transition temperatures to compare the various compounds. Clear-cut transition temperatures on their DSC thermograms were in good agreement with each other for the multiple heating/cooling cycles. The POM images and DSC thermograms show that most samples exhibit a stable nematic phase and a supercooled nematic phase. For example, Fig. 3 (b) and (c) display the typical marble texture of the nematic mesophase exhibited by **2TF2** in the heating/cooling scans. While a representative DSC thermogram shows that compound **2TF2** exhibits a crystal transition at 73.2 °C, a melting transition at 101.7 °C and a nematic to isotropic phase transition at 124.9 °C in the heating process in Fig. 3 (a). The heating/cooling scans note that the molecule **2TF2** shows enantiotropic nematic mesophase.

### Thermal properties

Fig. 4 illustrates the transition temperatures of compounds **nBF1**, **nBF2** and **nTF2**, in the heating process, as a function of the carbon number (n) in the alkyl chain. The melting and clearing points of them exhibited a clear even-odd effect. In contrast to **nBF1**, **nBF2** and **nTF2** with even terminal chain (n =2, 4) exhibited lower melting and clearing points than those with odd terminal chain (n =3, 5). Compared with **nBF2**, **nBF1** (n =3, 5) exhibited a lower melting point and a wider mesomorphic temperature range, which indicates that the lateral fluoro substituent on the first phenyl ring is more helpful in enhancing the stability of the mesophase.[16] Similarity with the literature[17], **3TF2** exhibits a lower melting point than that of **3T**.

As shown in Fig. 2, the introduction of the alkyne-bridge enhances the nematic mesomorphic temperature range and increased the clearing point temperature, because it cancels both the effects of angled benzene rings and the broadening of the molecule.[18] As observed in Fig. 5, the simulated molecular structures of **2BF2** and **2TF2** present that the fluorine-substituted biphenyl rings are twisted to about 39º, while the analogue molecule with the alkyne-bridge is flat.

A 1,3-dioxolane-terminated liquid crystal **5BF1** shows only an enantiotropic nematic phase, whereas the corresponding terminal alkenyl liquid crystal[12] showed enantiotropic nematic and smectic A phases. The phenomena can be attributed to the fact that the stability of mesophase is interrupted by the curved 1,3-dioxolane structure, which is more conducive to form a nematic phase. Meanwhile, we have noted that the 1,3-dioxolane terminal structure of **2BF2** exists

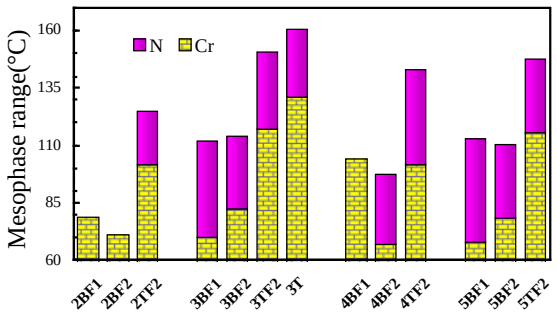


**Fig. 2** The mesophase range of compounds **nBF1**, **nBF2**, **nTF2 and 3T** during heating. Cr: crystal ; N: nematic LC phase interval.

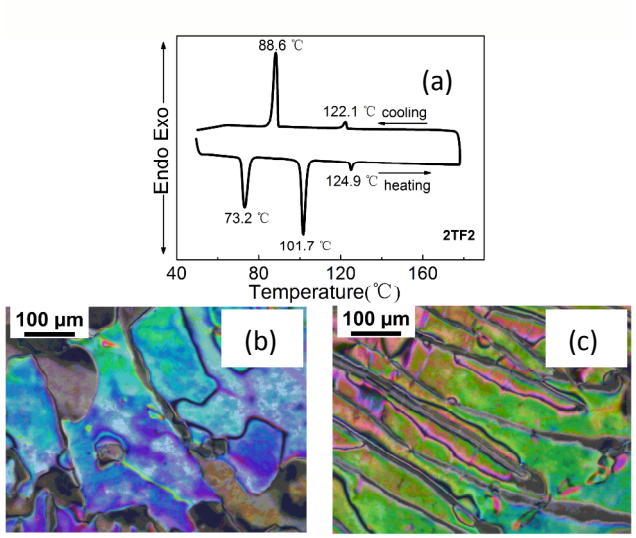


**Fig. 3** DSC trace (a) of **2TF2** and POM images (×200) of **2TF2**: marble texture of the nematic mesophase at 121 °C in the heating scan (b) and 116 °C in the cooling scan (c).

in a much curved molecular skeleton in Fig. 5, while the terminal alkyl or alkenyl shows a more linear structure.

### Physical properties

To clarify the correlations between the 1,3-dioxolane structure and the physical properties of LCs, reference compounds **2BF2V** and **3TR** were also prepared in Fig. 1.

Table 1 summarized the birefringence ($\Delta n$), dielectric anisotropy ($\Delta\varepsilon$) of compounds **2BF2**, **2TF2**, **3TF2**, **3T**, **2BF2V** and **3TR**. The $\Delta n$ , $\Delta\varepsilon$ of them were difficult to measure directly due to their higher melting points than 20 °C, herein 15 wt% of **2BF2**, **2TF2**, **3TF2**, **3T**, **2BF2V** or **3TR** was mixed with a positive mixture to measure by using guest–host method.[19] When all of the six compounds were respectively mixed in the same host mixture, the solubility experiments were carried out by observation if there was any crystal precipitation appeared at room temperature. After several weeks storage, none of them was observed to have any crystal precipitation, which indicates that these compounds have good solubility in the host mixture.

As shown in Table 1, the $\Delta\varepsilon$ of compound **3T** with 1,3-dioxolane

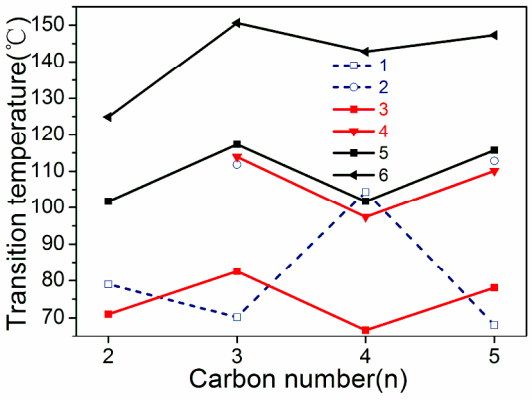


**Fig. 4** Transition behaviour of the compounds **nBF1** (C-N point for 1, N-I point for 2), **nBF2** (C-N point for 3, N-I point for 4) and **nTF2** (C-N point for, 5, N-I point for 6) series: dependence of the transition temperatures on the carbon number (n) of the terminal alkyl chain. C: crystal; N: nematic mesophase phase; I: isotropic liquid.

**Table 1.** The electro-optical properties[a] and DFT calculated principal components ($\alpha_{XX}$, $\alpha_{YY}$, $\alpha_{ZZ}$), isotropic component $\alpha$[b], anisotropy $\Delta\alpha$[c], dipole Moment ($\mu$) of compounds **2TF2**, **3TF2**, **3T**, **2BF2**, **2BF2V** and **3TR**.[d]

| compound | $\alpha_{XX}$ | $\alpha_{YY}$ | $\alpha_{ZZ}$ | $\alpha$[b] | $\Delta\alpha$[c] | $\mu$ | $\Delta n$[a] | $\Delta\varepsilon$[a] |
|---|---|---|---|---|---|---|---|---|
| **2TF2** | 623.3 | 271.0 | 193.0 | 362.4 | 391.3 | 1.56 | 0.2850 | 4.64 |
| **3TF2** | 639.6 | 279.8 | 203.4 | 374.3 | 398.0 | 1.61 | 0.2750 | 5.27 |
| **3T** | 639.6 | 279.4 | 201.4 | 373.5 | 399.2 | 1.08 | 0.3150 | 3.70 |
| **2BF2** | 472.3 | 256.4 | 193.9 | 307.5 | 247.2 | 2.03 | 0.1930 | 4.57 |
| **2BF2V** | 455.9 | 245.1 | 173.4 | 291.5 | 246.7 | 0.83 | 0.1900 | -1.51 |
| **3TR** | 611.8 | 265.4 | 193.8 | 357.0 | 382.2 | 0.27 | 0.2420 | 0.84 |

[a] Experimental measurement results. [b] $\alpha = (\alpha_{XX}+\alpha_{YY}+\alpha_{ZZ})/3$. [c] $\Delta\alpha = [\alpha_{XX} - (\alpha_{YY}+\alpha_{ZZ})/2]$.

[d] All polarizability components and the anisotropy parameter are expressed in Bohr ^3 (with 1 Bohr = 0.52917 Å).

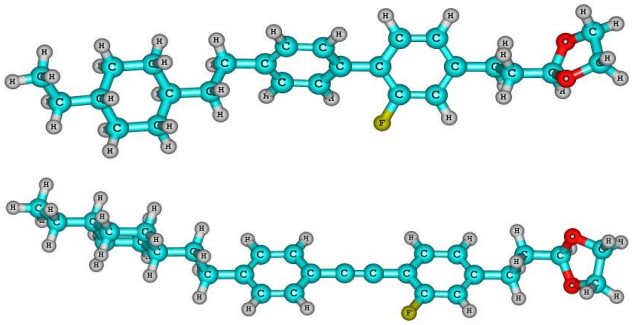

**Fig. 5** Molecular structures of compound **2BF2** (top) and **2TF2** (bottom) optimized at the DFT/b3lyp/6-31G (d, p) level of theory.

terminal is 3.7, in contrast to that of the alkyl compound **3TR**, where $\Delta\varepsilon$ is nearly zero. More particularly, the alkenyl liquid crystal **2BF2V** shows a negative $\Delta\varepsilon$ of -1.51, which is agree with the negative $\Delta\varepsilon$ reported by our group[20]. However, compound **2BF2** with 1,3-dioxolane terminal shows a positive $\Delta\varepsilon$ of 4.57. The above results reveal that the higher $\Delta\varepsilon$ value is strongly related to the 1,3-dioxolane terminal group. Meanwhile, the 1,3-dioxolane terminal group increases a ring structure to obtain LCs with a higher value of $\Delta n$. Thus, the 1,3-dioxolane terminal tolane-LCs **2TF2**, **3TF2** and **3T** possess a higher value of $\Delta n$ (0.28~0.32), which can be also attributed to the fact that the phenyl-tolane core increases the better π-electrons conjugation of the molecules. Moreover, the fluoro substituent is an electron-withdrawing group,[21] hence **3T** reveals a higher $\Delta n$ value than that of **3TF2**.

## DFT calculations

DFT computational studies based on quantum mechanical calculations were performed to gain more insight into the influence of the geometry, dipole moment ($\mu$) and polarizability on the nature of the $\Delta n$ and $\Delta\varepsilon$ properties, Table 1 summarizes the parameters from molecular **2BF2**, **2TF2**, **3TF2**, **3T**, **2BF2V** and **3TR**. Full geometry optimizations have been carried out without imposing any constraints using the Gaussian 09 program package.[22] Spin-restricted DFT calculations were carried out in the framework of the generalized gradient approximation (GGA) using B3LYP exchange-correlation functional and the 6-31G (d, p) basis set.[23] Based on the resulting geometries, harmonic vibrational frequencies were calculated at the same level of theory to confirm the reliability of optimized results. For example, the successful geometric data of molecular **2BF2** and **2TF2** are showed in the ESI† (see content 4).

On the molecular level, the birefringence of a nematic liquid crystal mostly depends on the polarisability anisotropy $\Delta\alpha$,[24] which can explain the numerical relationship of the $\Delta n$ for most compounds, but not for compound **3TF2** in Table 1. According to the Vuks equation[25] detailed in the ESI† (see content 5), for compound **2TF2** and **3TF2**, although the $\Delta\alpha$ values of them are very close, compound **2TF2** has lower $\alpha$ value than that of **3TF2**, which can explain why **2TF2** exhibits larger $\Delta n$ than that of **3TF2**. As observed in Table 1, while the lateral fluorine substituent increases the dipole moment, **3TF2** has naturally a higher dielectric anisotropy than that of **3T**. Compound **3TR** with the alkyl terminal group possesses a small dipole moment of 0.27, whereas the 1,3-dioxolane terminal group increases the dipole moment to 1.08, herein compound **3T** reveals a higher positive $\Delta\varepsilon$ of 3.7. At a low frequency, e.g. 1 kHz measured in this experiment, both the relative motions between molecules and the random motions of molecules themselves contribute together to the static dielectric anisotropy. The dielectric property strongly depends on the permanent dipole moment of molecules,[26] which can explain the numerical relationship of the $\Delta\varepsilon$ for most compounds.

However, compared with **2TF2**, **2BF2** possesses a higher value of $\mu$, but reveals a lower $\Delta\varepsilon$ value. We have noticed that dielectric parameters extrapolated for pure additives were analyzed using the Maier and Meier equation [eqn (1)][27-29], which includes molecular and phase parameters[30].

$$\Delta\varepsilon = \frac{NFh}{\varepsilon_0}\left\{\Delta\alpha - \frac{F\mu^2}{2k_BT}\left(1-3\cos^2\beta\right)\right\}S \qquad (1)$$

Although compound **2BF2** possesses a higher value of $\mu$, compound **2TF2** has larger $\Delta\alpha$ value than that of **2BF2**, which can explain why compound **2TF2** exhibits larger $\Delta\varepsilon$ than that of **2BF2**.

Besides, there is an exception to the positive $\Delta\varepsilon$ value in Table 1, which the alkenyl liquid crystal **2BF2V** shows a negative $\Delta\varepsilon$ of -1.51 in the host mixture. From the simulated molecular structure of **2BF2V**, we note that the total direction of the dipole moment to the Y axis results in the negative $\Delta\varepsilon$. (see Fig. S7 in the ESI†)

## Properties in the liquid crystal mixture

An approach to investigate the application of synthetic liquid crystal components was carried out by the formulation of liquid crystal mixture on basis of our previous system for the touch pannels. The compositions of the mixtures are detailed in the ESI† (see Table S2 and Table S3) and the procedure was reported in Ref [31]. **2BF2**, **3TF2** and **5BF1** were blended with SNULC-P01 by a replacement of **2H2BFB2V**, **3H2BFB2V** and **5H2BFB2V** in an almost same fraction to form SNULC-P02 mixture. The properties of the mixtures were measured by filling the sample into a liquid crystal cell with a thickness of 5 μm and the parameters are listed in Table 2. The new mixture SNULC-P02 displays a large $\Delta\varepsilon$ (4.34 vs 3.86) and thereby decreases the threshold voltage (1.39 vs 1.60). This significant improvement comfirmed that the synthetic components are promising candidates for wearable devices. Meanwhile, the broad

**Table 2.** Measured properties of the two LC mixtures at T = 25 °C, λ = 589 nm, and f = 1 kHz.

| No. | $\varepsilon_{/\!/}$ | $\varepsilon_{\perp}$ | $\Delta\varepsilon$ | $\Delta n$ | $\gamma_1$ (mPas) | $K_{11}$ (pN) | $V_{th}$ (V) | $T_r$ (ms) | $T_f$ (ms) | Mp (°C) | Cp (°C) |
|---|---|---|---|---|---|---|---|---|---|---|---|
| SNULC-P01 | 7.26 | 3.40 | 3.86 | 0.0764 | 81.6 | 8.4 | 1.60 | 8.5 | 10.5 | <-25 | 65.0 |
| SNULC-P02 | 7.67 | 3.33 | 4.34 | 0.0972 | 86.0 | 9.9 | 1.39 | 7.0 | 11.5 | <-30 | 67.1 |

nematic phase range and high birefingence are also characteristic in the mixture SNULC-P02.

## Conclusions

The 1,3-dioxolane terminal group has been identified as a highly effective structural building block that imparts a strongly positive dielectric anisotropy and birefringence in LCs compared with the same molecular skeleton. In contrast to the analogous materials with a buty-3-enyl terminal group, the 1,3-dioxolane substructure does not only increase the dipole moment, but it also improves the photostability. Meanwhile, the liquid crystal components with the 1,3-dioxolane terminal displayed a high value of $\Delta n$ (0.28~0.32) and positive $\Delta\varepsilon$ (3.7~5.3), which can correlate the DFT calculations well. The mixture SNULC-P02 with 1,3-dioxolane-terminated LCs showed a lower threshold voltage, wider nematic temperature range and higher birefringence than that of mixture SNULC-P01, which comfirmed further that our synthetic compounds are promising candidates for the wearable devices. By compared with the conventional methods to enhance the positive dielectric anisotropy, the use of 1,3-dioxolane as a terminal group delivers a facile and inexpensive pathway to reach the purpose. This pathway has a superiority and may provide a new strategy to design and synthesize novel liquid crystal materials with large dielectric anisotropy.

## Acknowledgements

The authors would like to thank the Defense Industrial Technology Development Program of China (B0520132007, B1120132028), Shaanxi National Science Foundation (2014JM7270), Key Technologies R&D Program of Xi'an (CXY1430(2)), the Key Technologies R&D Program of Shaanxi Province (2014K10-06), Program for Changjiang Scholars and Innovative Research Team in University (IRT-14R33) and the Fundamental Research Funds for the Central Universities (GK201504008, GK201501007, GK201501002) for financial support of this work. We are grateful to Professor Wenliang Wang at Shaanxi Normal University for theoretical calculations at Shaanxi Normal University.

## Notes and references

[a] Key Laboratory of Applied Surface and Colloid Chemistry, School of Materials Science and Engineering, Shaanxi Normal University, Xi'an 710119, China. E-mail: gmecazw@163.com; Fax: +86 29 8153 0702; Tel: +86 29 8153 0720

[b] Shaanxi University of Chinese Medicine, Xianyang, 712046, China.

[c] Xi'an Modern Chemistry Research Institute, Xi'an 710065, China.

† Electronic Supplementary Information (ESI) available: $^1$H NMR and $^{13}$C NMR spectra of target compounds. All characterized data. Table S1 and Fig. S6. The geometric data of molecular **2BF2** and **2TF2**. Vuks equation. The simulated molecular structure of **2BF2V.** Compositions of mixtures SNULC-P01 and SNULC-P02. See DOI: 10.1039/b000000x/

1 (*a*) S. H. Lee, S. S. Bhattacharyya, H. S. Jin and K. U. Jeong, *J. Mater. Chem.*, 2012, **22**, 11893−11903; (*b*) H. Khandelwal, R. C. G. M. Loonen, J. L. M. Hensen, A. P. H. J. Schenning and M. G. Debije, *J. Mater. Chem. A*, 2014, **2**, 14622−14627.

2 (*a*) Z. Luo, F. Peng, H. Chen, M. Hu, J. Li, Z. An and S. T. Wu, *Opt. Mater. Express*, 2015, **5**, 603−610; (*b*) H. Chen, M. Hu, F. Peng, J. Li, Z. An and S. T. Wu, *Opt. Mater. Express*, 2015, **5**, 655−660.

3 B. G. Kim, E. J. Jeong, J. W. Chung, S. Seo, B. Koo and J. Kim, *Nat. Mater*., 2013, **12**, 659−664.

4 (*a*) J. Ide, R. Mereau, L. Ducasse, F. Castet, H. Bock, Y. Olivier, J. Cornil, D. Beljonne, G. Davino, O. M. Roscioni and L. M. Zannoni, *J. Am. Chem. Soc*., 2014, **136**, 2911−2920; (*b*) B. Zhao, C. Z. Li, S. Q. Liu, J. J. Richards, C. C. Chueh, F. Ding, L. D. Pozzo, X. Li and A. K. Y. Jen, *J. Mater. Chem. A*, 2015, **3**, 6929−6934.

5 P. Kirsch and A. Hahn, *Eur. J. Org. Chem.*, 2005, 3095−3100.

6 P. Kirsch, M. Bremer, A. Taugerbeck and T. Wallmichrath, *Angew. Chem. Int. Ed.*, 2001, **40**, 1480−1484.

7 P. Kirsch, A. Hahn, R. Fröhlich and G. Haufe, *Eur. J. Org. Chem.*, 2006, 4819−4824.

8 P. Kirsch, W. Binder, A. Hahn, K. Jährling, M. Lenges, L. Lietzau, D. Maillard, V. Meyer, E. Poetsch, A. Ruhl, G. Unger and R. Fröhlich, *Eur. J. Org. Chem*., 2008, 3479−3487.

9 H. Zhang, S. Shiino, A. Shishido, A, Kanazawa, O. Tsutsumi, T. Shiono and T. Ikeda, *Adv. Mater*., 2000, **12**, 1336−1339.

10 M. O'Neill and S. M. Kelly, *Adv. Mater*., 2003, **15**, 1135−1146.

11 M. Tariq, S. Hameed, I. H. Bechtold, A. J. Bortoluzzi and A. A. Merlo, *J. Mater. Chem. C* , 2013, **1**, 5583−5593.

12 Y. Jiang, Z. An, P. Chen, X. Chen and M. Zheng, *Liq Cryst.*, 2012, **39**, 457−465.

13 R. Chen, Z. An, X. Chen and P. Chen, *Chem. J. of Chinese Universities.*, 2014, **35**, 1433−1438.

14 Y. Goto, K. Kitano and T. Ogawa, *Liq. Cryst.*, 1989, **5**, 225−232.

15 J. Li, X. Yang, N. Gan, B. Wu and Z. An, *Liq. Cryst.*, 2015, **42**, 397−403.

16 P. Balkwill, D. Bishop, A. Pearson and I. Sage, *Mol. Cryst. Liq. Cryst.*, 1985, **123**, 1−13.

17 M. Hird and K. J. Toyne, *Mol. Cryst. Liq. Cryst.*, 1998, **323**, 1−67.

18 J. Dziaduszek, P. Kula, R. Dąbrowski, W. Drzewiński, K. Garbat, S. Urban and S. Gauza, *Liq. Cryst.*, 2012, **39**, 239−247.

19 I. C. Khoo and S. T. Wu, Singapore: World Scientific; 1993.

20 Y. Jiang, L. Lu, P. Chen, X. Chen, J. Li and Z. An, *Liq Cryst.*, 2012, **39**, 957-963.

21 V. Reiffenrath, U. Finkenzeller, E. Poetsch, B. A. Rieger, D. Coates, J. W. Doane and Z. Yaniv, *Liq Cryst Disp Appl.*, 1990, **1257**, 84−94.

22 M. J. Frisch, G. W. Trucks, H. B. Schlegel, G. E. Scuseria, M. A. Robb, J. R. Cheeseman, G. Scalmani, V. Barone, B. Mennucci, G. A. Petersson, H. Nakatsuji, M. Caricato, X. Li, H. P. Hratchian, A. F. Izmaylov, J. Bloino, G. Zheng, J. L. Sonnenberg, M. Hada, M. Ehara, K. Toyota, R. Fukuda, J. Hasegawa, M. Ishida, T. Nakajima, Y. Honda, O. Kitao, H. Nakai, T. Vreven, J. A. Montgomery Jr, J. E. Peralta, F. Ogliaro, M. Bearpark, J. J. Heyd, E. Brothers, K. N. Kudin, V. N. Staroverov, R. Kobayashi, J. Normand, K. Raghavachari, A. Rendell, J. C. Burant, S. S. Iyengar, J. Tomasi, M. Cossi, N. Rega, J. M. Millam, M. Klene, J. E. Knox, J. B. Cross, V. Bakken, C. Adamo,J. Jaramillo, R. Gomperts, R. E. Stratmann, O. Yazyev, A. J. Austin, R. Cammi, C. Pomelli, J. W. Ochterski, R. L. Martin, K. Morokuma, V. G. Zakrzewski, G. A. Voth, P. Salvador, J. J.

Dannenberg, S. Dapprich, A. D. Daniels, Ö. Farkas, J. B. Foresman, J. V. Ortiz, J. Cioslowski and D. J. Fox, GAUSSIAN 09 (Revision B.01), Gaussian Inc., Wallingford, CT, 2010.

23 (*a*) K. Kim and K. D. Jordan, *J. Phys. Chem.*, 1994, **98**, 10089−10094; (*b*) P. J. Stephens, F. J. Devlin, C. F. Chabalowski and M. J. Frisch, *J. Phys. Chem.*, 1994, **98**, 11623−11627.

24 M. Hu, Z. An, J. Li, L. Mo, Z. Yang, J. Li, Z. Che and X. Yang, *Liq. Cryst.*, 2014, **41**, 1696−1702.

25 M. F. Vuks, *Opt Spectrosc.*, 1966, **20**, 361−368.

26 H. Ma, O. Hiroyoshi, S. Sigeru and T. Kazuhisa, *Chin. Phys. B*, 2010, **19**, 076104.

27 W. Maier and G. Meier, *Z. Naturforsch.*, 1961, **16A**, 262−267.

28 R. K. Nath, R. Deb, N. Chakraborty, G. Mohiuddin, R. D. S. Shankar and N. V. S. Rao, *J. Mater. Chem. C*, 2013, **1**, 663−670.

29 J. Pecyna, P. Kaszyński, B. Ringstrand and M. Bremer, *J. Mater. Chem. C*, 2014, **2**, 2956−2964.

30 P. Kaszyński, A. Januszko and K. L. Glab, *J. Phys. Chem. B*, 2014, **118**, 2238−2248.

31 S. T. Wu and C. S. Wu, *Phys. Rev. A*, 1990, **42**, 2219–2227.

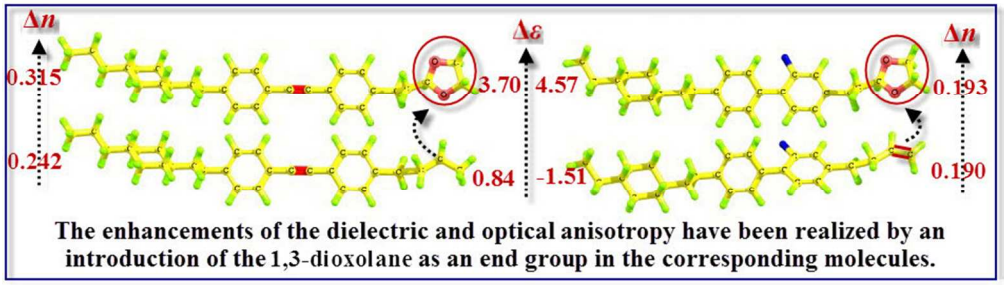


160x46mm (150 x 150 DPI)